

PHASE SEPARATION IN MODELS FOR MANGANITES: THEORETICAL ASPECTS AND COMPARISON WITH EXPERIMENTS*

E. Dagotto, S. Yunoki, and A. Moreo

National High Magnetic Field Lab and Department of Physics,
Florida State University, Tallahassee, FL 32306, USA

INTRODUCTION

Colossal magnetoresistance in metallic oxides such as $R_{1-x}X_x\text{MnO}_3$ (where $R = \text{La, Pr, Nd}$; $X = \text{Sr, Ca, Ba, Pb}$) is attracting considerable attention [1] due to its potential technological applications. A variety of experiments have revealed that oxide manganites have a rich phase diagram [2] with regions of antiferromagnetic (AF) and ferromagnetic (FM) order, as well as charge ordering, and a peculiar insulating state above the FM critical temperature T_c . Recently, *layered* manganite compounds $\text{La}_{1.2}\text{Sr}_{1.8}\text{Mn}_2\text{O}_7$ have also been synthesized [3] with properties similar to those of their 3D counterparts. Strong correlations are important for transition-metal oxides, and, thus, theoretical guidance is needed to understand the behavior of manganites and for the design of new experiments.

The appearance of ferromagnetism at low temperatures can be explained using the so-called Double Exchange (DE) mechanism [4, 5]. However, the DE model is incomplete to describe the entire phase diagram observed experimentally. For instance, the electron-phonon coupling may be crucial to account for the insulating properties above T_c [6]. The presence of a Berry phase at large Hund-coupling also challenges predictions from the DE model [7]. In a series of recent papers (Refs. [8, 9, 10, 11]) we have remarked that another phenomena occurring in manganites and not included in the DE description, namely the charge ordering effect, may be contained in a more fundamental Kondo-like model. More precisely, in those papers [8, 9, 10] it was reported the presence of *phase separation* (PS) between hole-undoped antiferromagnetic and hole-rich ferromagnetic regions in the low temperature phase diagram of the one-orbital FM Kondo model. In a recent paper by the same authors a similar phenomenon was also observed using two orbitals and Jahn-Teller phonons [11]. In this case the two phases involved are both spin ferromagnetic and the *orbital* degrees of freedom are responsible

*To appear in proceedings of the workshop “Physics of Manganites”, Michigan State University, July 26–29, 1998, eds. by T. A. Kaplan and S. D. Mahanti, Plenum Publishing Corporation.

for the phase separation. Upon the inclusion of long-range Coulombic repulsion, charge ordering in the form of non-trivial extended structures (such as stripes) could be stabilized, similarly as discussed for the cuprates [12, 13, 14, 15] but now also including ferromagnetic domains. The analysis carried out by our group suggests that phenomena as rich as observed in the high-Tc superconductors may exist in the manganites as well, and hopefully our effort will induce further theoretical and experimental work in this context.

The present paper should be considered as an informal review of the present status of the computational studies of models for manganites that reported the existence of phase separation at low temperatures. It does *not* pretend to be a comprehensive article, and thus we encourage the readers to consult the literature mentioned here to find out additional references. The paper is organized as follows: in the next section the results for the case of the one-orbital Kondo model are reviewed, with emphasis on the phase diagram. Most of the calculations are performed with classical t_{2g} -spins but results for quantum spins are also shown. In addition, models that interpolate between Cu-oxides and Mn-oxides have also been studied, as well as the influence on our conclusions of Coulomb interactions beyond the on-site term. In the following section results recently reported for the case of the two-orbital model with Jahn-Teller phonons are described. Once again the main emphasis is given to the phase diagram. In both of those previous sections the main result is that tendencies to ferromagnetism and phase-separation are in strong competition in these models. Such a phenomenon appears so clearly in all dimensions of interest and for such a wide range of models that it leads us to believe that it may be relevant for experiments in the context of manganites. A discussion of experimental literature that have reported some sort of charge inhomogeneity compatible with phase separation (after Coulomb interactions are added) are briefly described towards the end of the paper. In the last section a summary is provided.

ONE ORBITAL FERROMAGNETIC KONDO MODEL

Results for Classical t_{2g} -Spins

The FM Kondo Hamiltonian [4, 16] is defined as

$$H = -t \sum_{\langle ij \rangle \sigma} (c_{i\sigma}^\dagger c_{j\sigma} + h.c.) - J_H \sum_{i\alpha\beta} c_{i\alpha}^\dagger \sigma_{\alpha\beta} c_{i\beta} \cdot \mathbf{S}_i, \quad (1)$$

where $c_{i\sigma}$ are destruction operators for one species of e_g -fermions at site \mathbf{i} with spin σ , and \mathbf{S}_i is the total spin of the t_{2g} electrons, assumed localized. The first term is the e_g electron transfer between nearest-neighbor Mn-ions, $J_H > 0$ is the Hund coupling, the number of sites is L , and the rest of the notation is standard. The density is adjusted using a chemical potential μ . In this section and Refs. [8, 9] the spin \mathbf{S}_i is considered classical (with $|\mathbf{S}_i| = 1$), unless otherwise stated. Although models beyond Eq.(1) may be needed to fully understand the manganites (notably those that include lattice effects as studied later in this paper), it is important to analyze in detail the properties of simple Hamiltonians to clarify if part of the experimental rich phase diagram can be accounted for using purely electronic models.

To study Eq.(1) in the t_{2g} -spin classical limit a Monte Carlo (MC) technique was used: first, the trace over the e_g -fermions in the partition function was carried out

exactly diagonalizing the $2L \times 2L$ Hamiltonian of electrons in the background of the spins $\{\mathbf{S}_i\}$, using library subroutines. The fermionic trace is a positive function of the classical spins and the resulting integration over the two angles per site parametrizing the \mathbf{S}_i variables can be performed with a standard MC algorithm without “sign problems”. In addition, part of the calculations of Refs. [8, 9] were also performed with the Dynamical Mean-Field approximation ($D=\infty$) [16], the Density-Matrix Renormalization Group (DMRG), and the Lanczos method. Special care must be taken with the boundary conditions (BC) [17, 18].

Our results are summarized in the phase diagram of Fig.1. In 1D (and also in 2D, not shown) and at low temperatures clear indications of (i) ferromagnetism, (ii) spin incommensurate (IC) correlations, and (iii) phase separation were identified. Results are also available in small 3D clusters and qualitatively they agree with those in Fig.1. The same occurs working at $D = \infty$ (see Refs. [8, 9]). In 1D we also obtained results with quantum t_{2g} -spins $S=3/2$ (shown below) which are in good agreement with Fig.1.

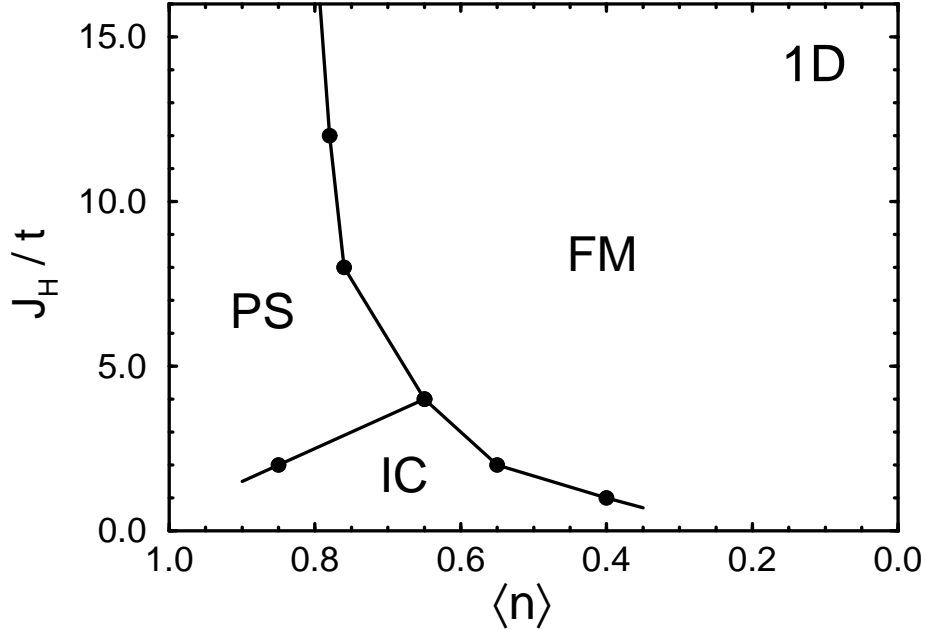


Figure 1: Phase diagram of the FM Kondo model reported in Refs. [8, 9] obtained using numerical techniques. FM, IC, and PS denote regimes with FM correlations, spin incommensurate correlations, and with phase separation between undoped AF and hole-rich FM regions, respectively. The results shown correspond to one dimension and they were obtained with MC simulations at $T = t/75$ using chains with $L=20, 30$ and 40 sites. This result is taken from Refs. [8, 9].

The boundaries of the FM region of the phase diagram were found evaluating the spin-spin correlation defined as $S(\mathbf{q}) = (1/L) \sum_{\mathbf{j}, \mathbf{m}} e^{i(\mathbf{j}-\mathbf{m}) \cdot \mathbf{q}} \langle \mathbf{S}_{\mathbf{j}} \cdot \mathbf{S}_{\mathbf{m}} \rangle$. Fig.2 shows $S(\mathbf{q})$ at zero momentum vs. T/t for typical examples in 1D and 2D. The rapid increase of the spin correlations as T is reduced and as the lattice size grows clearly points towards the existence of ferromagnetism in the system [19]. It is natural to assume that the driving force for FM in this context is the DE mechanism. Repeating this procedure for a variety of couplings and densities, the robust region of FM shown in Fig.1 was determined. In

the small J_H/t region IC correlations were observed monitoring $S(\mathbf{q})$ [20]. Both in 1D and 2D there is one dominant peak which moves away from the AF location at $\langle n \rangle = 1$ towards zero momentum as $\langle n \rangle$ decreases. In the 2D clusters the peak moves from (π, π) towards $(\pi, 0)$ and $(0, \pi)$, rather than along the main diagonal. Note that our computational study predicts IC correlations only in the small and intermediate J_H/t regime.

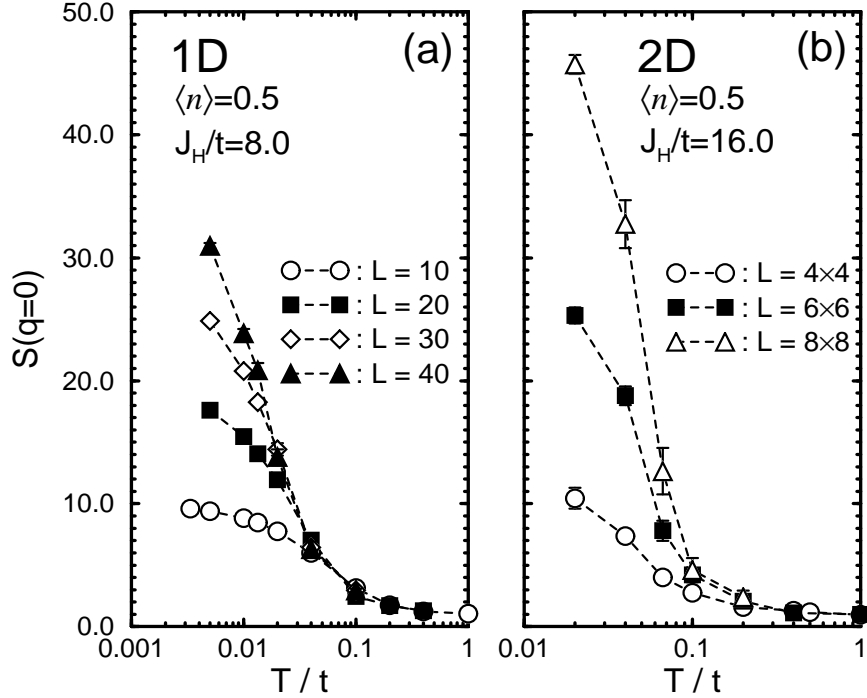


Figure 2: Spin-spin correlations of the classical spins at zero momentum $S(\mathbf{q} = 0)$ vs temperature T (in units of t). MC results for several lattice sizes are shown on (a) chains and (b) 2D clusters. The density and coupling are shown. In (a) closed shell BC are used i.e. periodic BC for $L = 10$ and 30 and antiperiodic BC for $L = 20$ and 40 . In (b) open BC are used. Results taken from Ref. [8].

The main result of Refs. [8, 9] is contained in Fig.3 where the computational evidence for the existence of phase separation in dimensions 1, 2, and ∞ is given. The presence of a discontinuity in $\langle n \rangle$ vs μ shows that some electronic densities can not be stabilized by tuning the chemical potential [21]. If the system is nominally prepared with such density it will spontaneously separate into two regions with the densities corresponding to the extremes of the discontinuities of Fig.3. By analyzing these extremes the properties of the two domains can be studied. One region is undoped ($\langle n \rangle = 1$) with strong AF correlations, while the other contains all the holes and the spin-spin correlations between the classical spins are FM (see the inset of Fig.3a. The results are similar in $D=2$ and infinite). This is natural since holes optimize their kinetic energy in a FM background. On the other hand, at $\langle n \rangle = 1$ the DE mechanism is not operative: if the electrons fully align their spins they cannot move in the conduction band due to the Pauli principle. Then, energetically an AF pattern is formed. As J_H grows, the jump in Fig.3 is reduced and it tends to disappear in the $J_H = \infty$ limit.

Experimentally, PS may be detectable using neutron diffraction techniques, since

$S(q)$ should present a two peak structure, one located at the AF position and the other at zero momentum. Since this also occurs in a canted ferromagnetic state care must be taken in the analysis of the experimental data. Another alternative is that Coulombic forces prevent the macroscopic accumulation of charge intrinsic of a PS regime. Thus, microscopic hole-rich domains may develop in the manganites, perhaps in the form of stripes.

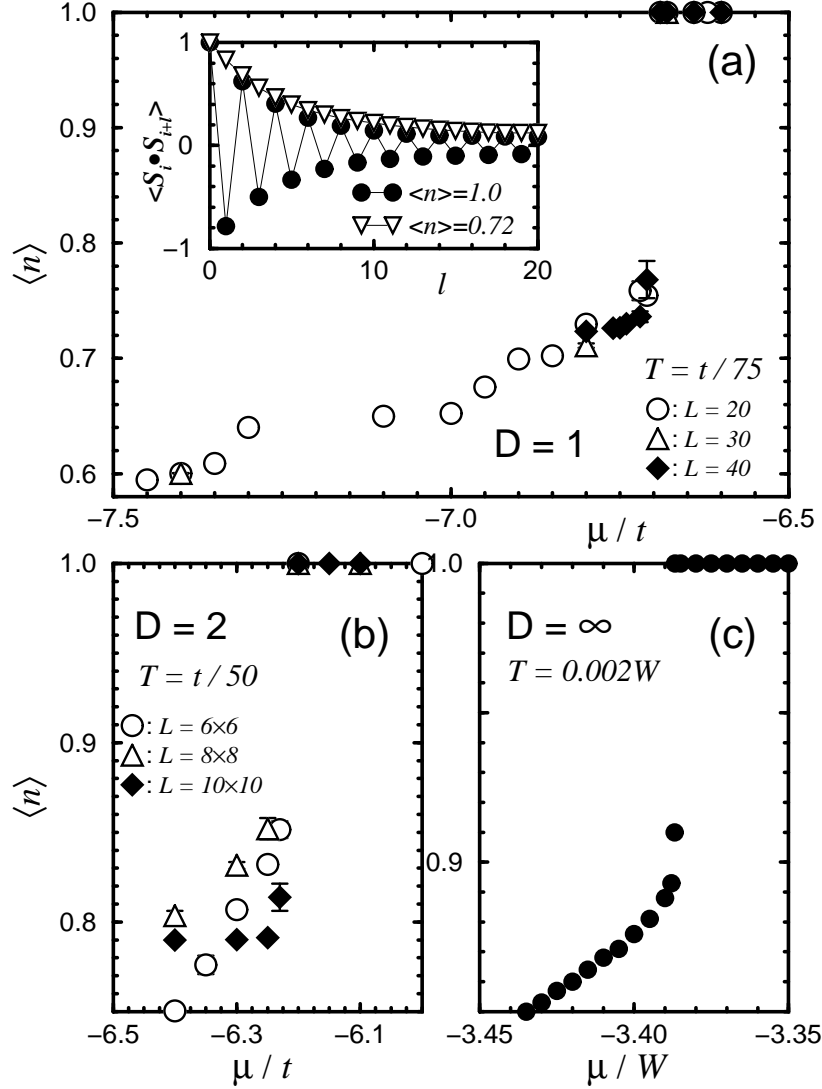


Figure 3: Electronic density $\langle n \rangle$ vs chemical potential μ in (a) $D=1$, (b) $D=2$, and (c) $D = \infty$ clusters. Temperatures are indicated. The coupling is $J_H/t = 8.0$ in (a) and (b) and $J_H/W = 4.0$ in (c) (for the definition of W see Ref. [8]). PBC were used both in $D=1$ and 2. The discontinuities shown in the figures are indicative of PS. In (a) the inset contains the spin-spin correlation in real space at densities 1.0 and 0.72 showing that indeed PS occurs between AF and FM regions. The results are taken from Refs. [8, 9] where more details can be found.

Although the phase diagram of Fig.1 has PS close to half-filling, actually this phenomenon also occurs at $\langle n \rangle \sim 0$ if an extra direct AF exchange interaction between the localized spins is included [10]. This coupling may be originated in a small hopping amplitude for the t_{2g} electrons. At $\langle n \rangle = 0$, model Eq.(1) supplemented by a Heisen-

berg coupling J'/t among the localized spins produces an AF phase, as in experiments, which upon electron doping induces a competition between AF (with no e_g -electrons) and FM electron-rich regions, similarly as for $\langle n \rangle = 1$ but replacing holes by electrons. Thus, PS or charge ordering could exist in manganites both at large and small fermionic densities. A careful study of the influence of the J' coupling on the phase diagram of the 1-orbital Kondo model has been recently presented in Ref. [10]

For completeness, upper bounds on the 3D critical temperature T_c were also provided in Refs. [8, 9]. Using MC simulations in principle it is possible to calculate T_c accurately. However, the algorithm used in our studies prevented us from studying clusters larger than 6^3 even at $J_H = \infty$. In spite of this limitation, monitoring the spin-spin correlations in real space allows us to judge at what temperature T^* the correlation length reaches the boundary of the 6^3 cluster. Since the bulk T_c is smaller than T^* , this gives us upper bounds for the critical temperature. Following this procedure at $\langle n \rangle = 0.5$, it was found that for $T \sim 0.1t$ robust correlations reach the boundary, while for $T \geq 0.12t$ the correlation is short-ranged. Thus, at this density we estimate that $T_c < 0.12t$. Since results for the e_g electrons bandwidth range from $BW \sim 1 \text{ eV}$ [22] to $BW \sim 4 \text{ eV}$ [23], producing a hopping $t = BW/12$ between 0.08 and 0.33 eV, then the estimations for the critical temperature of Refs. [8, 9] range roughly between $T_c \sim 100 \text{ K}$ and 400 K . This is within the experimental range and in agreement with other results [16, 24]. Then, in principle purely electronic models can account for T_c .

Quantum t_{2g} -Spins: Phase Diagram

In the previous section we have used classical localized spins to simplify the technical aspects of the computational study and since the realistic values of those spins is large ($3/2$). However, it is interesting to study the phase diagram for the case of quantum t_{2g} -spins at least in one special case, in order to verify that indeed the use of classical spins is a good approximation. Using the Lanczos and DMRG techniques, the phase diagram for the cases of t_{2g} -spins $S = 3/2$ and $1/2$ was reported in Refs. [8, 9] for the case of one dimension, and one of them is shown in Fig. 4. The techniques used work in the canonical ensemble, instead of grand-canonical as the MC simulation of the previous section. The presence of phase separation is investigated here using the compressibility (which if it becomes negative signals the instability of the density under study). Fig. 4 shows that the three regimes found before (namely PS, FM, and IC) are also observed in the quantum case. The results for $S = 3/2$ are even quantitatively similar to those found with the MC technique of the previous section, while those for $S = 1/2$ are only qualitatively similar. The overall conclusion is that the use of classical t_{2g} -spins in the Ferromagnetic Kondo Model was found to be a good approximation, and no important differences in the phase diagram have been observed (at least in this one-dimensional example) when quantum spins are used. Studies in dimensions larger than one would be too involved using quantum localized spins, and thus the similarities between the classical and quantum cases found here help us to investigate those more realistic dimensions.

Models for Other Transition-Metal Oxides

In the previous sections we have found that models for manganites analyzed with reliable unbiased techniques provide a phase diagram where there are two main phases in competition: a ferromagnetic regime and a “phase-separated” regime (actually the latter is not a phase but a region of unstable densities). Such a clear result suggest that

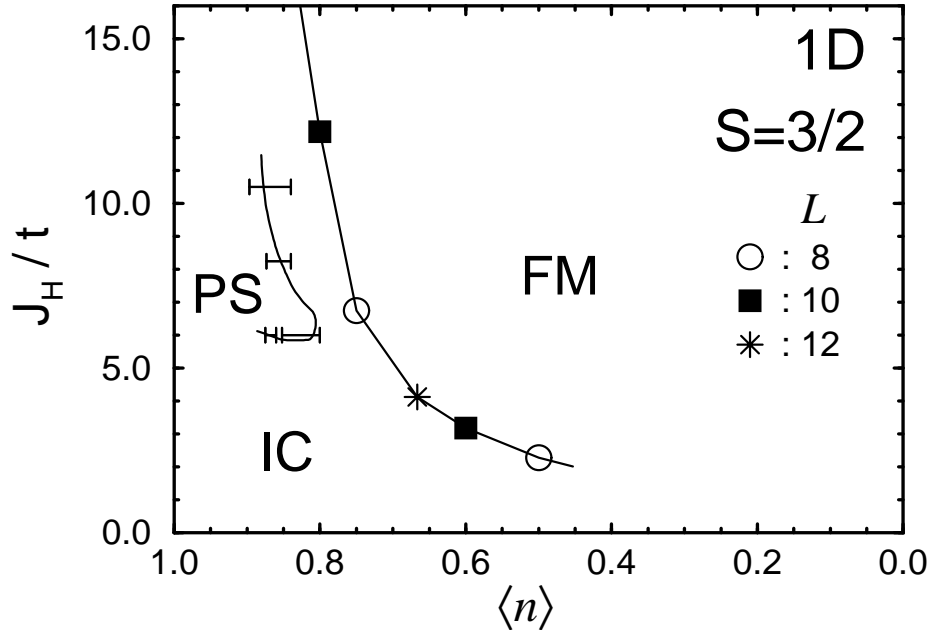


Figure 4: Phase diagram of the Ferromagnetic Kondo model using quantum t_{2g} -spins. The results correspond to a localized spin of value $S = 3/2$ (normalized as $|S| = 1$, see Ref. [9]). The notation is the same as in Fig.1. The techniques used to obtain the results are Lanczos and DMRG. The result is taken from Ref. [9].

the phenomenon maybe more general than expected. Actually recent studies of models for transition-metal oxides in general [17], in the limit of a large Hund-coupling, revealed phase diagrams where indeed FM and PS dominated. Let us consider the evolution of such a phase diagram as we move in the periodic table of elements from copper, to nickel, etc, eventually arriving to manganese. The study of Ref. [17] was carried out in one-dimension for technical reasons, but nevertheless the tendencies observed are strong enough to be valid in other dimensions as well. For the case of copper the model used was the plain “t-J” model, namely a model where we have spins of value $S = 1/2$ and holes which carry no spin. The phase diagram in this case was known for a long time. It contains no indications of ferromagnetism (at least no “clear” indications), and there is phase separation only at large J/t . However, the study of Ref. [17] for Ni-oxides using a t-J-like model with “spins” of value $S = 1$ and “holes” with spin $S = 1/2$ (since they correspond to the removal of one electron of a Ni-site) revealed that both FM and PS are clearly enhanced in the phase diagram with respect to the case of Cu-oxides. The technical details can be found in Ref. [17]. As the spin grows these tendencies become stronger and actually for the case of the Mn-oxides only a small window separates the fully polarized FM and PS regimes. This result suggests that the phenomenon is very general and should be searched for in other transition-metal oxides as well.

Influence of Coulomb Interactions

The accumulation of charge that occurs in the phase separation regime described in the previous section is not stable once Coulombic interactions beyond the on-site

term are added to the problem. It is expected that in the presence of these long-range interactions the ground state will have clusters of one phase embedded into the other (droplet regime). However, a computational study including these Coulomb interactions is very difficult. For instance, the analysis of model Eq.(1) would require a Hubbard-Stratonovich decomposition of the fermionic interaction which not only introduces more degrees of freedom, but in addition the infamous “sign problem” which will prevent the study from being carried out at low enough temperatures. Then, only techniques such as Lanczos or DMRG can handle properly this type of models. Recently, the analysis including Coulombic terms started by using the “minimum” possible Hamiltonian, namely the 1-orbital Ferromagnetic Kondo Model with localized spin-1/2 and with the addition of an on-site Coulomb term and a nearest-neighbor (NN) density-density V -coupling that penalizes the accumulation of charge in two NN sites [25]. The results are still being analyzed so here only a qualitative summary will be presented.

The conclusions of the study of Malvezzi et al [25]. thus far are the following: (1) the on-site coupling U apparently does not affect qualitatively the results found at $U = 0$ as long as the Hund-coupling is large; (2) in the regime of phase separation near $\langle n \rangle = 1$ the addition of a V -term produces results compatible with the cluster formation anticipated in the previous paragraph. Actually even at finite V in a regime where the compressibility shows that phase separation no longer exists (i.e. all densities are stable), clear remnants of such a PS regime are found. For instance, at $V = 0$ the spin structure factor $S(q)$ has robust peaks at both $q = 0$ and π . Introducing V , these peaks still exist but they move slightly from the 0 and π positions forming incommensurate structures; (3) in the regime where at $V = 0$ there is ferromagnetism induced by a double-exchange process, the inclusion of a nonzero coupling V transforms the ground state into a FM charge-density-wave (CDW). In this phase the spins are aligned but the charge is not uniformly distributed. The overall phase diagram is rather complicated. We are actively working in this context to analyze the qualitative aspects of such a result. But it is already clear that charge-ordering tendencies are observed at all densities upon introducing V , in agreement with experiments. More detailed results will be presented soon.

TWO ORBITALS AND JAHN-TELLER PHONONS

Phase Diagram

In spite of the rich phase diagram observed in the study of the 1-orbital Ferromagnetic Kondo Model in the previous section and its similarities with experiments, there are aspects of the real manganites that require a more sophisticated approach. For instance, dynamical Jahn-Teller (JT) distortions are claimed to be very important [6], and a proper description of the recently observed orbital order [26] obviously needs at least two orbitals. Such a multi-orbital model with JT phonons is nontrivial, and thus far it has been studied only using the dynamical mean-field approximation [27]. The previous experience with the 1-orbital case suggests that a computational analysis is actually crucial to understand its properties. In addition, it is conceptually interesting to analyze whether the PS described before [8, 9, 10] exists also in multi-orbital models.

The first computational study of a 2-orbital model for manganites including JT phonons was reported recently by the authors in Ref. [11] and here a summary of the main conclusions will be discussed. The results show a rich phase diagram including

a novel regime of PS induced by the *orbital*, rather than the spin, degrees of freedom (DOF). The Hamiltonian used in that study had three contributions $H_{KJT} = H_K + H_{JT} + H_{AF}$. The first term is

$$H_K = - \sum_{\langle \mathbf{ij} \rangle \sigma ab} t_{ab} (c_{i\alpha\sigma}^\dagger c_{j\beta\sigma} + h.c.) - J_H \sum_{i\alpha\beta} \mathbf{S}_i \cdot c_{i\alpha}^\dagger \sigma_{\alpha\beta} c_{i\beta}, \quad (2)$$

where $\langle \mathbf{ij} \rangle$ denotes nearest-neighbor lattice sites, $J_H > 0$ is the Hund coupling, the hopping amplitudes t_{ab} are described in Ref. [28], $a, b = 1, 2$ are the two e_g -orbitals, the t_{2g} spins \mathbf{S}_i are assumed to be classical (with $|\mathbf{S}_i| = 1$) since their actual value in Mn-oxides (3/2) is large [29], and the rest of the notation is standard. None of the results described below depends crucially on the set $\{t_{ab}\}$ selected [28]. The energy units are chosen such that $t_{11} = 1$ in the x -direction. In addition, since J_H is large in the real manganites, here it will be fixed to 8 (largest scale in the problem) unless otherwise stated. The e_g -density $\langle n \rangle$ is adjusted using a chemical potential μ .

The coupling with JT-phonons is through [6, 30]

$$H_{JT} = \lambda \sum_{i\alpha b\sigma} c_{i\alpha\sigma}^\dagger Q_i^{ab} c_{ib\sigma} + \frac{1}{2} \sum_i (Q_i^{(2)^2} + Q_i^{(3)^2}), \quad (3)$$

where $Q_i^{11} = -Q_i^{22} = Q_i^{(3)}$, and $Q_i^{12} = Q_i^{21} = Q_i^{(2)}$. These phonons are assumed to be classical, which substantially simplifies the computational study. This is a reasonable first approximation towards the determination of the phase diagram of the H_{KJT} model. Finally, a small coupling between the t_{2g} -spins is needed to account for the AF character of the real materials even when all La is replaced by Ca or Sr (fully doped manganites). This classical Heisenberg term is $H_{AF} = J' \sum_{\langle \mathbf{ij} \rangle} \mathbf{S}_i \cdot \mathbf{S}_j$, where J' is fixed to 0.05 throughout the paper, a value compatible with experiments [31]. To study H_{KJT} a Monte Carlo (MC) technique similar to that employed in Refs. [8, 9, 10] and in the previous section for the 1-orbital problem was used. Finally, to analyze orbital correlations the pseudospin operator $\mathbf{T}_i = \frac{1}{2} \sum_{\sigma ab} c_{i\alpha\sigma}^\dagger \sigma_{ab} c_{ib\sigma}$ was used, while for spin correlations the operator is standard. The Fourier-transform of the pseudospin correlations is defined as $T(\mathbf{q}) = \frac{1}{L} \sum_{\mathbf{l}, \mathbf{m}} e^{i\mathbf{q} \cdot (\mathbf{l} - \mathbf{m})} \langle \mathbf{T}_{\mathbf{m}} \cdot \mathbf{T}_{\mathbf{l}} \rangle$, with a similar definition for the spin structure factor $S(\mathbf{q})$.

Let us first consider the limit $\langle n \rangle = 1.0$, corresponding to undoped manganites. Fig.5 shows $T(q)$ and $S(q)$ at representative momenta $q = 0$ and π vs. λ . For small electron-phonon coupling the results are similar to those at $\lambda = 0.0$, namely a large $S(0)$ indicates a tendency to spin-FM order induced by DE (as in the qualitatively similar 1-orbital problem at $\langle n \rangle = 0.5$ [8]). The small values of $T(q)$ imply that in this regime the orbitals remain disordered. When the coupling reaches $\lambda_{c1} \sim 1.0$, the rapid increase of $T(\pi)$ now suggests that the ground state has a tendency to form a *staggered* (or “antiferro” AF) orbital pattern, with the spins remaining FM aligned since $S(0)$ is large. The existence of this phase was discussed before, but using multi-orbital Hubbard models with Coulomb interactions and without phonons [32]. Our results show that it can be induced by JT phonons as well. As the coupling increases further, another transition at $\lambda_{c2} \sim 2.0$ occurs to a spin-AF orbital-FM state ($S(\pi)$ and $T(0)$ are large). In this region a 1-orbital approximation is suitable.

The three regimes of Fig.5 can be understood in the limit where λ and J_H are the largest scales, and using $t_{12} = t_{21} = 0$, $t_{11} = t_{22} = t$ for simplicity. For parallel spins with orbitals split in a staggered (uniform) pattern, the energy per site at lowest order in t is $\sim -t^2/\Delta$ (~ 0), where Δ is the orbital splitting. For antiparallel spins with uniform (staggered) orbital splitting, the energy is $\sim -t^2/2J_H$ ($\sim -t^2/(2J_H + \Delta)$).

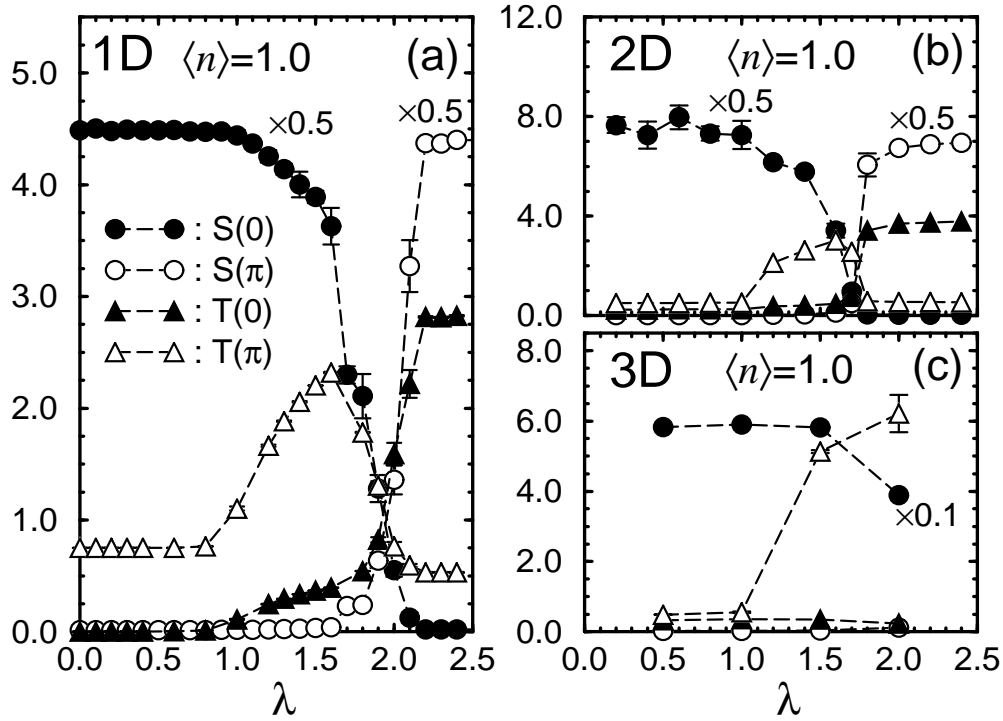


Figure 5: (a) $T(q)$ and $S(q)$ vs λ , working at $\langle n \rangle = 1.0$, $T = 1/75$, $J_H = 8$, $J' = 0.05$, and in 1D with 10 sites. $\{t_{ab}\}$ correspond to set T_1 (see [28]). Results with sets T_2 and T_3 are qualitatively the same; (b) Same as (a) but for a 4^2 cluster, $T = 1/50$, and hopping T_3 (T_4) in the y (x) direction. $q = 0(\pi)$ denotes $(0, 0)$ $((\pi, \pi))$; (c) Same as (a) but for a 4^3 cluster, $T = 1/50$, the 3D hopping amplitudes of Ref. [28], and $J_H = \infty$. $q = 0(\pi)$ denotes $(0, 0, 0)$ $((\pi, \pi, \pi))$. These results were taken from Ref. [11].

Then, when $\Delta < 2J_H$ (“intermediate” λ s), a spin-FM orbital-AF order dominates, while as λ grows further a transition to a spin-AF orbital-FM ground state is expected. Note that this reasoning is actually valid in any dimension. To confirm this prediction, results for a 2D cluster in Fig.5b are shown. Indeed the qualitative behavior is very similar to the 1D results. In 3D (Fig.5c), where studies on 4^3 clusters can only be done at $J_H = \infty$ to reduce the number of DOF, at least two of the regimes of Fig.5a have been identified [33].

Let us discuss the transport properties in the three regimes at $\langle n \rangle = 1$. The algorithm used in Ref. [8, 11] allow us to calculate *real-time* dynamical responses accurately, including the optical conductivity $\sigma(\omega > 0)$, since all the eigenvectors in the fermionic sector for a given spin and phonon configuration are obtained exactly. From the sum-rule, e_g kinetic-energy, and the integral of $\sigma(\omega > 0)$, the $\omega = 0$ Drude-weight D_W can be obtained. Carrying out this calculation it was observed that D_W vanishes at λ_{c1} signaling a *metal-insulator* transition (MIT). Here the insulating phase is spin-FM and orbital-AF, while the metallic one is spin-FM and orbital-disordered [34]. The density of states (DOS) for $\lambda > \lambda_{c1}$ was also calculated in Ref. [11] and it presents a clear gap at the Fermi level. The qualitative shape of D_W vs λ on 4^2 and 4^3 clusters was found to be the same as in 1D and, thus, it is reasonable to assume that the MIT exists also in all dimensions of interest.

Consider now the influence of hole doping on the $\langle n \rangle = 1.0$ phase diagram, with

special emphasis on the stability of other densities as μ is varied. Fig.6 shows $\langle n \rangle$ vs μ in the intermediate- λ regime. It is remarkable that *two* regions of unstable densities exist at low- T (similar conclusions were reached using the Maxwell's construction [35]). These instabilities signal the existence of PS in the H_{KJT} model. At low-density there is separation between an (i) empty e_g -electron band with AF-ordered t_{2g} -spins and a (ii) metallic spin-FM orbital uniformly ordered phase. This regime of PS is analogous to the spin-driven PS found at low-density in the 1-orbital problem [10]. On the other hand, the unstable region near $\langle n \rangle = 1.0$ is *not* contained in the 1-orbital case. Here PS is between the phase (ii) mentioned above, and (iii) the insulating intermediate- λ spin-FM and orbital-AF phase described in Fig.5 [36]. In 2D the results were found to be very similar (Ref. [11]). The driving force for this novel regime of PS are the *orbital* degree of freedom, since the spins are uniformly ordered in both phases involved. Studying $\langle n \rangle$ vs μ , for $\lambda < \lambda_{c1}$ only PS at small densities is observed, while for $\lambda > \lambda_{c2}$ the PS close to $\langle n \rangle = 1$ is similar to the same phenomenon observed in the 1-orbital problem since it involves a spin-AF orbital-FM phase [8].

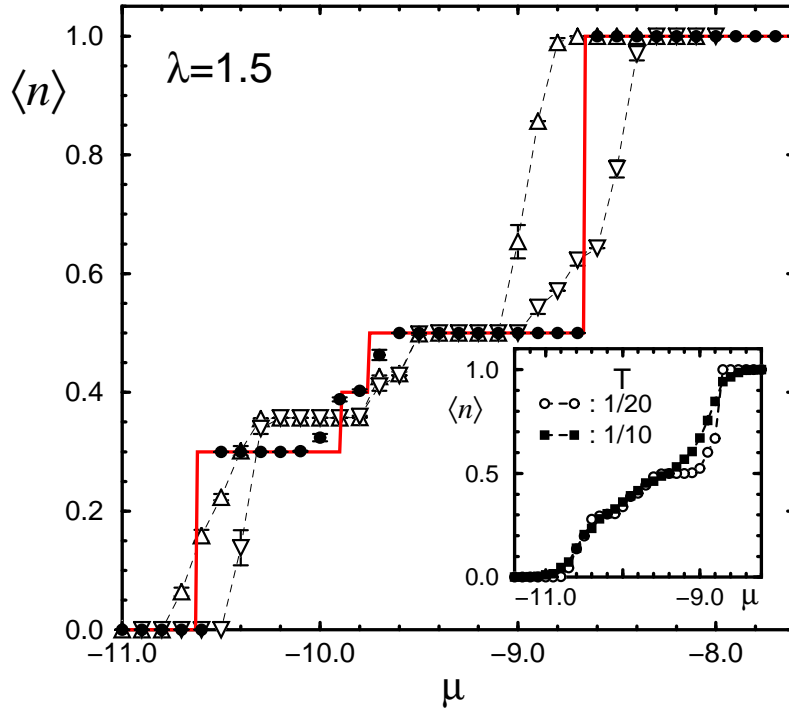


Figure 6: $\langle n \rangle$ vs μ at $\lambda = 1.5$, $L = 10$, and $T = 1/40$ (solid circles). The discontinuities near $\langle n \rangle = 1.0$ and 0.0 show the existence of unstable densities. The solid line is obtained from the Maxwell's construction. The triangles are results also at $\lambda = 1.5$ and $T = 1/40$, but using 14 sites and only 2×10^4 MC sweeps to show the appearance of *hysteresis* loops as in a first-order transition. The inset shows the T -dependence of the results at $L = 10$. These results were taken from Ref. [11].

The phase diagram of the 1D H_{KJT} model is given in Fig.7. The two PS regimes are shown, together with the metallic spin-FM region. This phase is separated into two regions, one ferro-orbital ordered and the other orbitally disordered. The existence of these two regimes can be deduced from the behavior of the pseudospin correlations, the mean value of the pseudospin operators, and the probability of double occupancy of

the same site with different orbitals. The results are similar for several $\{t_{ab}\}$ sets [28]. The simulations of Ref. [11] suggest that the qualitative shape of Fig.7 should be valid also in $D = 2$ and 3. Recently we learned of experiments where the low- T coexistence of domains similar to those described in Ref. [11], i.e. one orbitally-ordered and the other FM-metallic, has been observed in Mn-perovskites [37, 38].

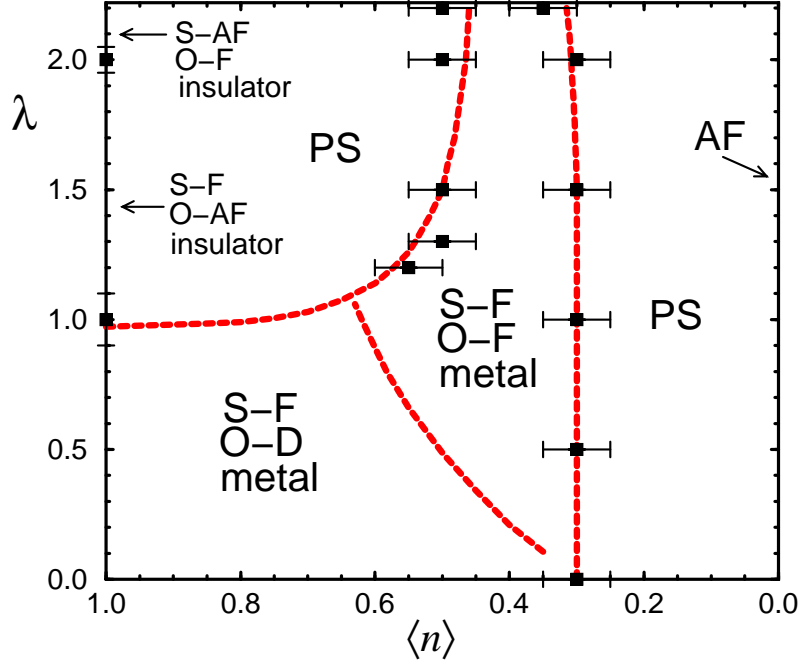


Figure 7: Phase diagram of the H_{KJT} model at low- T , $J_H = 8.0$, $J' = 0.05$, and using set T_1 for $\{t_{ab}\}$. S – F and S – AF denote regimes with FM- and AF-spin orders, respectively. O – D, O – F, and O – AF represent states with disordered, uniform and staggered orbital orders, respectively. PS means phase separation. These results were taken from Ref. [11].

Optical Conductivity

In Ref. [11] results for $\sigma(\omega)$ were also presented. Experimental studies for a variety of manganites such as $\text{Nd}_{0.7}\text{Sr}_{0.3}\text{MnO}_3$, $\text{La}_{0.7}\text{Ca}_{0.3}\text{MnO}_3$, and $\text{La}_{0.7}\text{Sr}_{0.3}\text{MnO}_3$ reported a broad peak at $\omega \sim 1\text{eV}$ (for hole doping $x > 0.2$ and $T > T_c^{FM}$) [39, 40]. At room- T there is negligible weight near $\omega = 0$, but as T is reduced the 1eV -peak shifts to smaller energies, gradually transforming into a Drude response well below T_c . The finite- ω peak can be identified even inside the FM phase. The coherent spectral weight is only a small fraction of the total. Other features at larger energies $\sim 3\text{eV}$ involve transitions between the J_H -split bands and the O -ions. In addition, Jung et al. [40] interpreted the 1eV feature at room- T as composed of two peaks due to intra- and inter-atomic transitions in JT-distorted environments.

In Fig.8, $\sigma(\omega)$ for the H_{KJT} model is shown at $\langle n \rangle = 0.7$ and several temperatures near the unstable PS region of Fig.7 (weight due to J_H split bands occurs at higher energy). Here the FM spin correlation length grows rapidly with the lattice size for $T^* \leq 0.05t$, which can be considered as the “critical” temperature. Both at high- and intermediate- T a broad peak is observed at $\omega \sim 1$, smoothly evolving to

lower energies as T decreases. The peak can be identified well-below T^* as in experiments [39, 40]. Eventually at very low- T , $\sigma(\omega)$ is dominated by a Drude peak. The T -dependence shown in the figure is achieved at this λ and $\langle n \rangle$ by a combination of a finite- ω phonon-induced broad feature that loses weight, and a Drude response that grows as T decreases (for smaller λ s, the two peaks can be distinguished even at low- T). The similarity with experiments suggests that real manganites may have couplings close to an unstable region in parameter space. In the inset, D_W vs T is shown. Note that at $T \sim T^*$, D_W vanishes suggesting a MIT, probably due to magneto polaron localization. Results for the 1-orbital case are smoother, with no indications of a singularity. These features are in agreement with experiments, since the manganite “normal” state is an insulator. Work is currently in progress to analyze in more detail this MIT transition.

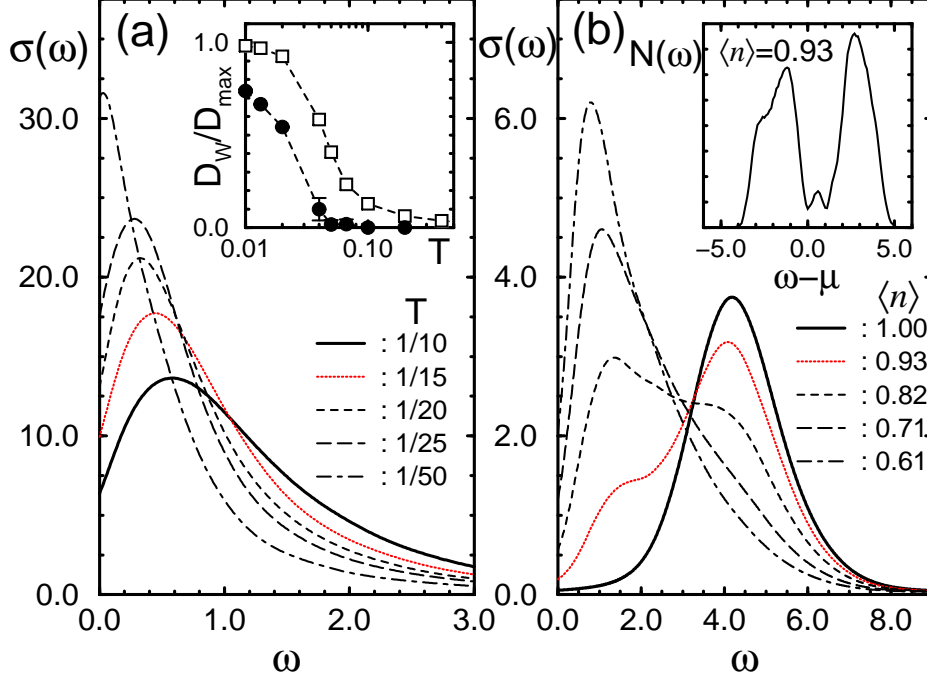


Figure 8: (a) $\sigma(\omega)$ parametric with T , at $\lambda = 1.0$, $\langle n \rangle = 0.7$, and $L = 20$. The inset shows D_W vs T for both the H_{KJT} (solid circles) and the 1-orbital model of Ref. [8] (open squares) (the latter at $\langle n \rangle = 0.65$). D_W is normalized to its maximum value at $T = 0.01$; (b) $\sigma(\omega)$ vs ω parametric with $\langle n \rangle$ at $\lambda = 1.5$, $T = 1/10$, and $L = 16$ (results for $L = 10$ are very similar). The inset shows the lower J_H -split DOS at $\langle n \rangle = 0.93$. Both in (a) and (b) a δ -function broadening $\epsilon = 0.25$ was used. These results were taken from Ref. [11].

A similar good agreement with experiments was observed working in the regime of the orbitally-induced PS but at a temperature above its critical value T_{PS} (roughly $\sim 1/20$, see inset Fig.6). Here the broad feature observed at high- T in Fig.8a moves to higher energies (Fig.8b) since λ has increased. At the temperature of the plot the system is an insulator at $\langle n \rangle = 1$, but as hole carriers are added a second peak at lower energies develops, in addition to a weak Drude peak (which carries, e.g., just 1% of the total weight at $\langle n \rangle = 0.61$). This feature at high- T is reminiscent of recent experimental results [40] where a two-peak structure was observed at room- T and several densities. Similar results were obtained on 4^2 clusters. In Fig.8b the peak at large- ω is caused by phononic effects since its position was found to grow rapidly with λ . It corresponds

to intersite transitions between Mn^{3+} JT-split states. The lower energy structure is compatible with a Mn^{3+} - Mn^{4+} transition [41]. The inset of Fig.8b shows the DOS of the system. The two peaks above μ are responsible for the features found in $\sigma(\omega)$. This interpretation is the same as given in Ref. [27] at $D = \infty$.

EXPERIMENTAL CONSEQUENCES OF PHASE SEPARATION

A large number of papers in the context of experimental studies of manganites have reported the presence of some sort of inhomogeneity in the system that is tempting to associate with the phase-separation tendencies observed in our studies. In the next paragraph we will mention some of these results such that the interested reader can have at hand at least part of the relevant references on the subject to decide by him/herself on this issue.

Some of the experiments that have reported results that could be compatible with ours are the following (in a random order): **1.** De Teresa et al. [42] studied $\text{La}_{1-x}\text{Ca}_x\text{MnO}_3$ using small-angle neutron scattering, magnetic susceptibility and other techniques, at $x=1/3$. The analysis of their data showed the existence of “magnetic clusters” of size approximately 12\AA above the ferromagnetic critical temperature; **2.** Hennion et al. [43] recently presented elastic neutron scattering results below T_c at $x = 0.05$ and 0.08 also for $\text{La}_{1-x}\text{Ca}_x\text{MnO}_3$. They interpreted their results as indicative of “magnetic droplets”. The density of these droplets was found to be much smaller than the density of holes implying that each droplet contains several holes; **3.** Lynn and collaborators [44] have studied $\text{La}_{1-x}\text{Ca}_x\text{MnO}_3$ at $x=1/3$ also using neutron scattering. Lattice anomalies and magnetic irreversibilities near T_c were interpreted as evidence of two coexisting distinct phases; **4.** Perring et al. [31] studying $\text{La}_{1.2}\text{Sr}_{1.8}\text{Mn}_2\text{O}_7$ with neutron scattering reported the presence of long-lived antiferromagnetic clusters coexisting with ferromagnetic critical fluctuations above T_c ; **5.** Allodi et al. [45] using NMR applied to $\text{La}_{1-x}\text{Ca}_x\text{MnO}_3$ at $x \sim 0.1$ observed coexisting resonances corresponding to FM and AF domains; **6.** Cox et al. [46] studying $\text{Pr}_{0.7}\text{Ca}_{0.3}\text{MnO}_3$ with x-ray and powder neutron scattering reported the presence of ferromagnetic clusters; **7.** Bao et al. [47] in their analysis of $\text{Sr}_{2-x}\text{La}_x\text{MnO}_4$ (2D material) found phase separation at small e_g -densities; **8.** Yamada et al. [48] in their study of $\text{La}_{1-x}\text{Sr}_x\text{MnO}_3$ with neutron scattering at $x=0.1$ and 0.15 interpreted their results as corresponding to polaron ordering; **9.** Roy et al. [49] studying $\text{La}_{1-x}\text{Ca}_x\text{MnO}_3$ near $x = 0.50$ found the coexistence of two carrier types: nearly localized carriers in the charge-ordered state and a parasitic population of free carriers tunable by stoichiometry; **10.** Booth et al. [50] also studying $\text{La}_{1-x}\text{Ca}_x\text{MnO}_3$ found that the number of delocalized holes n_{dh} in the ferromagnetic phase changes with the magnetization M as $\ln(n_{dh}) \propto -M$. Since the magnetization saturates well below T_c , this implies that there is a range of temperatures where sizable fractions of localized and delocalized holes coexist; **11.** Jaime et al. [51] reported the possibility of polaronic distortions of the paramagnetic phase of $\text{La} - \text{Ca} - \text{Mn} - \text{O}$ manganites persisting into the ferromagnetic phase, and analyzed the data with a two-fluid model; **12.** Zhou and Goodenough [52] studying the thermopower and resistivity of $^{16}\text{O}/^{18}\text{O}$ isotope-exchanged $(\text{La}_{1-x}\text{Nd}_x)_{0.7}\text{Ca}_{0.3}\text{MnO}_3$ found indications of a segregation of hole-rich clusters within a hole-poor matrix in the paramagnetic state; **13.** Billinge et al. [53] reported the coexistence of localized and delocalized carriers in a wide range of densities and temperatures below T_c ; **14.** Ibarra et al. [54] studied $(\text{La}_{0.5}\text{Nd}_{0.5})_{2/3}\text{Ca}_{1/3}\text{MnO}_3$ concluding that insulating charge-ordered and metallic ferromagnetic regions coexist at low temperatures; **15.** Rhyne et al. [55] in their study of $\text{La}_{0.53}\text{Ca}_{0.47}\text{MnO}_3$ with neutron

diffraction found two magnetic phases below the transition temperature, one ferromagnetic and the second antiferromagnetic, both persisting down to 10K; **16.** Heffner et al. [56] studying $\text{La}_{0.67}\text{Ca}_{0.33}\text{MnO}_3$ using zero-field muon spin relaxation and resistivity techniques found indications of polarons on the spin and charge dynamics; **17.** Jung et al. [57] have very recently studied the optical conductivities of $\text{La}_{7/8}\text{Sr}_{1/8}\text{MnO}_3$ concluding that there are indications in this system of phase separation.

The common theme of these experiments, and possibly others that have escaped our attention, is that some sort of inhomogeneity appears in the analysis of the data. The phenomenon is apparently more clear at small hole densities x and low temperatures which is precisely the region where our results indicate a strong tendency to phase separate. But also above T_c in the interesting densities around $x=1/3$ magnetic clusters have been reported. It is nothing but natural to imagine a “smooth” connection between $x \sim 0.1$ and low temperature with $x \sim 1/3$ and temperatures above T_c . In this case the large droplets found by Hennion et al. [43] could have evolved as to become the magnetic clusters of De Teresa et al. [42] by a reduction of their size and number of holes inside. We strongly encourage experimental work that could contribute to the answer of this or other important issues around the common theme of possible charge segregation in real manganites.

SUMMARY

Summarizing, a comprehensive computational study of models for manganites have found that the expected double-exchange induced strong tendencies to ferromagnetic correlations at low temperatures are in competition with a regime of “phase separation”. This regime was identified in all dimensions of interest, using one and two orbitals (the latter with Jahn-Teller phonons), and both with classical and quantum localized t_{2g} spins. It also appears in the presence of on-site Coulomb interactions. This robustness of our results suggests that phase separation may also be present in real manganites. In the previous section experimental literature that have reported some form of charge inhomogeneity in the context of the manganites has been briefly reviewed. It is concluded that theory and experiments seem to be in qualitative agreement and phase separation tendencies (which may correspond to the formation of magnetic droplets or even stripes once Coulomb interactions beyond the on-site term are included in the analysis) should be taken seriously. They may even be responsible for the phenomenon of Colossal Magnetoresistance that motivated the current enormous interest in the study of manganites in the first place!

ACKNOWLEDGEMENTS

E. D. and A. M. are supported by the NSF grant DMR-9520776. S. Y. thanks the NHMFL for support.

References

- [1] S. Jin et al., Science **264**, 413 (1994); J. M. D. Coey, M. Viret, and S. von Molnar, *Mixed Valence Manganites*, Adv. Phys. (1998), in press.

- [2] P. E. Schiffer, A. P. Ramirez, W. Bao, and S-W. Cheong, Phys. Rev. Lett. **75**, 3336 (1995); A. P. Ramirez et al., Phys. Rev. Lett. **76**, 3188 (1996); C. H. Chen and S-W. Cheong, Phys. Rev. Lett. **76**, 4042 (1996); S-W. Cheong and C. H. Chen, in *Colossal Magnetoresistance and Related Properties*, ed. by B. Raveau and C. N. R. Rao (World Scientific).
- [3] Y. Moritomo, A. Asamitsu, H. Kuwahara, Y. Tokura, Nature **380**, 141 (1996).
- [4] C. Zener, Phys. Rev. **82**, 403 (1951).
- [5] P. G. de Gennes, Phys. Rev. **118**, 141 (1960).
- [6] A. J. Millis, et al., Phys. Rev. Lett. **74**, 5144 (1995); H. Röder, et al., Phys. Rev. Lett. **76**, 1356 (1996).
- [7] E. Müller-Hartmann and E. Dagotto, Phys. Rev. **B 54**, R6819 (1996).
- [8] S. Yunoki, J. Hu, A. Malvezzi, A. Moreo, N. Furukawa, and E. Dagotto, Phys. Rev. Lett. **80**, 845 (1998).
- [9] E. Dagotto, S. Yunoki, A. Malvezzi, A. Moreo, J. Hu, S. Capponi, D. Poilblanc, and N. Furukawa, Phys. Rev. **B 58**, 6414 (1998).
- [10] S. Yunoki and A. Moreo, Phys. Rev. **B 58**, 6403 (1998).
- [11] S. Yunoki, A. Moreo, and E. Dagotto, cond-mat/9807149.
- [12] V. J. Emery, S. A. Kivelson, and H. Q. Lin, Phys. Rev. Lett. **64**, 475 (1990). See also V. J. Emery, and S. A. Kivelson, Physica **C 209**, 597 (1993).
- [13] E. Dagotto, Rev. Mod. Phys. **66**, 763 (1994), and references therein.
- [14] J. M. Tranquada et al., Nature **375**, 561 (1995), and references therein.
- [15] U. Löw et al., Phys. Rev. Lett. **72**, 1918 (1994); S. Haas et al., Phys. Rev. **B 51**, 5989 (1995).
- [16] N. Furukawa, J. Phys. Soc. Jpn. **63**, 3214 (1994).
- [17] J. Riera, K. Hallberg, and E. Dagotto, Phys. Rev. Lett. **79**, 713 (1997).
- [18] Closed shell BC or open BC are needed to stabilize a ferromagnet. If other BC are used the spin correlations at short distances are still strongly FM (if working at couplings where ferromagnetism is stable), but not at large distances where they become negative. This well-known effect was observed before in K. Kubo, J. Phys. Soc. Jpn. **51**, 782 (1982); J. Zang, et al., J. Phys.: Condens. Matter **9**, L157 (1997); T. A. Kaplan and S. D. Mahanti, *ibid*, L291 (1997); and in Ref. [17]. It does not present a problem in the analysis shown in this paper.
- [19] In both 1D and 2D the Mermin-Wagner theorem forbids a nonzero T_c in the model. However, the correlation lengths can be very large even at finite T/t .
- [20] IC effects were predicted using a Hartree-Fock approximation (J. Inoue and S. Maekawa, Phys. Rev. Lett. **74**, 3407 (1995)) as an alternative to canted FM [5].

- [21] See also E. L. Nagaev, Phys. Status Solidi (b) **186**, 9 (1994); D. Arovas and F. Guinea, cond-mat/9711145; M. Yu. Kagan, et al., cond-mat/9804213; M. Yamanka, W. Koshibae, and S. Maekawa, cond-mat/9807173.
- [22] Y. Moritomo, A. Asamitsu and Y. Tokura, Phys. Rev. **B 51**, 16491 (1995).
- [23] D. D. Sarma et al., Phys. Rev. **B 53**, 6873 (1996).
- [24] H. Röder, et al., Phys. Rev. **B 56**, 5084 (1997).
- [25] A. Malvezzi, S. Yunoki, and E. Dagotto, cond-mat/9809281.
- [26] Y. Murakami et al., Phys. Rev. Lett. **80**, 1932 (1998).
- [27] A. J. Millis et al., Phys. Rev. **B 54**, 5405 (1996).
- [28] Most of the work in one-dimension (1D) has been performed using $t_{11} = t_{22} = 2t_{12} = 2t_{21}$ (set T_1), but results have also been obtained with $t_{11} = t_{22}$ and $t_{12} = t_{21} = 0$ (T_2), as well as with the hopping that takes into account the proper orbital overlap, namely $t_{11} = 3t_{22} = \sqrt{3}t_{12} = \sqrt{3}t_{21}$ (T_3) (see S. Ishihara et al., Phys. Rev. **B 56**, 686 (1997)). In two-dimensions (2D), the set T_1 in both directions was used, but also the combination of T_3 in the y -direction and $t_{11} = 3t_{22} = -\sqrt{3}t_{12} = -\sqrt{3}t_{21}$ (T_4) in the x -direction. Finally, in three-dimensions (3D) T_4 was used in the x -direction, T_3 in the y -direction, and $t_{11} = t_{12} = t_{21} = 0$, $t_{22} = 4/3$ (T_5) in the z -direction.
- [29] This approximation was shown to be accurate in Ref. [8, 9].
- [30] J. Kanamori, J. Appl. Phys. (Suppl.) **31**, 145 (1960).
- [31] T. G. Perring et al., Phys. Rev. Lett. **78**, 3197 (1997).
- [32] J. B. Goodenough, Phys. Rev. **100**, 565 (1955); K. I. Kugel and D. I. Khomskii, JETP Lett. **15**, 446 (1972); S. Ishihara, J. Inoue and S. Maekawa, Phys. Rev. **B 55**, 8280 (1997); T. Mizokawa and A. Fujimori, Phys. Rev. **B 56**, R493 (1997).
- [33] Studies at larger values of λ 's are too costly in CPU time.
- [34] In Ref. [27], a MIT at $\lambda \sim 1$ was also found but it was not associated with orbital order.
- [35] The energies needed for this construction are obtained at low- T from the MC evolution of the density [10].
- [36] Slave-fermion mean-field studies of a model with strong Coulomb interactions and no JT phonons by S. Maekawa et al. (private communication) have also recently observed a similar PS pattern.
- [37] P. G. Radaelli et al., talk given at the *Second International Conference on Stripes and High T_c Superconductivity*, Rome, June 2-6 (1998). The results of Ref. [11] were presented at the same conference session by one of the authors (A.M.).

- [38] Recently calculations in the infinite dimensional limit of the two orbital Kondo model with Coulomb interactions have been presented (T. Momoi and K. Kubo, Phys. Rev. **B 58**, R567 (1998)). A reexamination of these results have found a phase separation regime for this model (K. Kubo, private communication, to be published). Thus, the effect discussed in computational studies of the two-orbital problem with JT phonons (Refs. [8] and [11]) is likely to survive the inclusion of realistic Coulomb interactions.
- [39] M. Quijada et al., cond-mat/9803201. See also S. G. Kaplan et al., Phys. Rev. Lett. **77**, 2081 (1996); Y. Okimoto et al., Phys. Rev. Lett. **75**, 109 (1995) and Phys. Rev. **B 55**, 4206 (1997); T. Ishikawa et al., Phys. Rev. **B 57**, R8079 (1998).
- [40] J. H. Jung et al., Phys. Rev. **B 57**, R11043 (1998); K. H. Kim et al., cond-mat/9804167 and 9804284.
- [41] Although its dependence with λ was weak.
- [42] J. M. De Teresa et al., Nature (London) **386**, 256 (1997).
- [43] M. Hennion et al., Phys. Rev. Lett. **81**, 1957 (1998)
- [44] J. W. Lynn et al., Phys. Rev. Lett. **76**, 4046 (1996).
- [45] G. Allodi et al., Phys. Rev. **B 56**, 6036 (1997); Phys. Rev. **B 57**, 1024 (1998).
- [46] D. E. Cox et al., Phys. Rev. **B 57**, 3305 (1998).
- [47] Wei Bao et al., Solid State Comm. **98**, 55 (1996).
- [48] Y. Yamada et al., Phys. Rev. Lett. **77**, 904 (1996).
- [49] M. Roy, J. F. Mitchell, A. P. Ramirez, and P. Schiffer, Phys. Rev. **B 58**, 5185 (1998).
- [50] C. H. Booth, F. Bridges, G. H. Kwei, J. M. Lawrence, A. L. Cornelius, and J. J. Neumeier, Phys. Rev. Lett. **80**, 853 (1998); Phys. Rev. **B 57**, 10440 (1998).
- [51] M. Jaime, P. Lin, M. B. Salamon, P. Dorsey, and M. Rubinstein, cond-mat/9808160.
- [52] J.-S. Zhou and J. B. Goodenough, Phys. Rev. Lett. **80**, 2665 (1998).
- [53] S. J. L. Billinge, R. G. DiFrancesco, G. H. Kwei, J. D. Thompson, M. F. Hundley, and J. Sarrao, proceedings of the workshop "Physics of Manganites", Michigan State University, July 1988, Eds. T. Kaplan and S. D. Mahanti (this volume).
- [54] M. R. Ibarra, G.-M. Zhao, J. M. De Teresa, B. Garcia-Landa, Z. Arnold, C. Marquina, P. A. Algarabel, H. Keller, and C. Ritter, Phys. Rev. **B 57**, 7446 (1998).
- [55] J. J. Rhyne, H. Kaiser, H. Luo, Gang Xiao, and M. L. Gardel, J. Appl. Phys. **93**, 7339 (1998).
- [56] R. H. Heffner et al., Phys. Rev. Lett. **77**, 1869 (1996).
- [57] J. H. Jung, K. H. Kim, H. J. Lee, J. S. Ahn, N. J. Hur, T. W. Noh, M. S. Kim, and J.-G. Park, cond-mat/9809107.